Reversible Spatiotemporal Control of Induced Protein Degradation by Bistable photoPROTACs

Patrick Pfaff [1], Kusal T. G. Samarasinghe[2], Craig M. Crews[2,3,4] and Erick M. Carreira[1]

[1], ETH Zürich, Vladimir-Prelog-Weg 3, HCI, 8093 Zürich, Switzerland

[2], Dept of Molecular, Cell, and Developmental Biology, Yale University, New Haven, CT 06511

[3], Dept of Chemistry, Yale University, New Haven, CT 06511

[4], Dept of Pharmacology, Yale University, New Haven, CT 06511

Abstract. Off-target effects are persistent issues of modern inhibition-based therapies. By merging the strategies of photopharmacology and small molecule degraders, we introduce a novel concept for persistent spatiotemporal control of induced protein degradation that potentially prevents off-target toxicity. Building on the successful principle of bifunctional all-small molecule Proteolysis Targeting Chimeras (PROTACs), we designed photoswitchable PROTACs (**photoPROTACs**) by including *ortho*-F_4-azobenzene linkers between both warhead ligands. This highly bistable yet photoswitchable structural component leads to reversible control over the topological distance between both ligands. The *azo*-*cis*-isomer is observed to be inactive because the distance defined by the linker is prohibitively short to permit complex formation between the protein binding partners. By contrast, the *azo*-*trans*-isomer is active because it can engage both protein partners to form the necessary and productive ternary complex. Importantly, due to the bistable nature of the *ortho*-F_4-azobenzene moiety employed, the photostationary state of the **photoPROTAC** is persistent, with no need for continuous irradiation. This technique offers reversible on/off switching of protein degradation that is compatible with an intracellular environment and, therefore, could be vastly useful in experimental probing of biological signaling pathways – especially those crucial for oncogenic signal transduction. Additionally, this strategy may be suitable for therapeutic implementation in a wide variety of disease phenotypes. By enabling reversible activation and deactivation of protein degradation, **photoPROTACs** offer advantages over conventional photocaging strategies that irreversibly release active agents.

Introduction. In recent years, the transition from inhibition of aberrant protein function to specific degradation of undesired proteins with **Pro**teolysis **Ta**rgeting **C**himeras (PROTACs) has resulted in remarkable progress and is currently effecting a paradigm shift in drug discovery and therapy development.[1,2] PROTACs affect highly efficient protein degradation by commandeering the endogenous processes of the ubiquitin-proteasome system. PROTACs engage proteins of interest and E3 ligases in a ternary complex, leading to specific polyubiquitination and labelling of proteins for degradation via the proteasome. This approach has allowed quick expansion of the "druggable proteome" beyond proteins that bear distinct functional sites responsible for their respective mode of action. By avoiding high drug doses and acting via novel mechanisms, PROTACs show promise as therapeutic candidates for disease phenotypes that display resistance to conventional inhibition-based therapy.[3]

With the evolution from peptide- to small-molecule based PROTACs, the therapeutic potential of PROTACs is quickly expanding. Selective degradation of transcriptional regulators (BRD4[4,5], CDK9[6], TRIM24[7]), trans-membrane receptor tyrosine kinases (EGFR[8], c-Met[8], ALK[9]), hormone receptors (ER, AR)[10] or proteins linked to neurodegenerative diseases (Tau[11]) extended the potential of PROTACs for treatment of a variety of diseases, such as cancer of the hematopoietic tissue[12] or hormone receptor-mediated solid malignancies.[13] Recent additions to the portfolio of chimeric degraders include functional molecules specifically targeting degradation of extracellular proteins.[14,15]

In spite of the tremendous advancements outlined, current PROTAC approaches may still have off-target effects because systemic application can affect untargeted tissue, a disadvantage shared with traditional inhibitor-based therapeutics. As an example, ARV-771, a highly active BET protein degrader, has been shown to achieve complete regression of prostate cancer in a CRPC mouse xenograft model.[13] However, a general cytotoxic effect was also observed, most notably with the occurrence of skin deterioration at the injection site. This demonstrates the need for a switchable element within the PROTAC scaffold allowing to reversibly turn degradation on and off in a spatiotemporal manner.

A strategy to potentially circumvent off-target effects of PROTACs involves the use of designed peptides, known as phosphoPROTACs, that can be conditionally activated via phosphorylation by specific growth-factor stimuli.[16] Other approaches couple light stimuli to irreversibly induce protein degradation. This includes photocaging[17] and the use of inducible degrons.[18] However, both of those techniques require the fusion of protein domains. Nonetheless, the use of light stimuli is a highly attractive approach due to the high spatiotemporal precision with which it can be applied.[19] Yet, there is a need for light-based strategies complementing optogenetic approaches. In this regard, the growing field of photopharmacology includes many examples enabling optical control of receptor function by employment of photoswitchable ligands.[20,21] This prompted us to evaluate possible ways of introducing a photoswitchable handle within the PROTAC scaffold.

Rationale. Despite the published work with a variety of small molecules, linkers within PROTACs have been the subject of only nominal variation, which most often has been restricted to alkyl and polyether linkers of varying lengths. This has led to observations that highlight the subtle sensitivity of ternary complex formation to linker length and composition.[22,23] Analysis of the small-molecule PROTAC literature suggests that a minimum linker length is necessary between the warheads, because shorter linkers are otherwise unable to span the gap needed to bind the recruited proteins in a ternary complex.

The critical difference in linker length between active and inactive degraders in many of the reported examples is about 3 Å.[3,24] Strikingly, the switch between *trans*- and *cis*-azobenzenes corresponds to a very similar difference of 3-4 Å in topological distance. Making use of this observation, we envisioned generation of photoswitchable PROTACs (**photoPROTACs**) in which the typical linear polyether linker is replaced by azobenzenes. This would serve to generate trifunctional PROTACs that include two ligands and a photoswitchable element within the degrader scaffold. At the heart of the idea is the design of a ***trans*-photoPROTAC** that corresponds to the

optimized linker length for efficient induction of ternary complex formation between POI and E3 ligase (**Figure 1A**). By contrast, the photoswitched ***cis*-photoPROTAC** would span a prohibitively short distance and thus be unable to reach the binding pocket of the second binding partner, precluding ternary complex formation, ubiquitination and eventual degradation.

In considering the potential applications, the ideal photoswitchable PROTAC-based therapeutic would have long-lived photostationary states (~ days) that are populated following initial light stimuli and persist throughout the treatment, avoiding continued or pulsed irradiation exposure. This requires the design of inactive *azo-cis*-isomers that are configurationally stable in biological settings. In this respect, bistable *ortho*-tetrafluoroazobenzenes (*o*-F_4-azobenzenes) have been recently introduced[25] and their *azo-cis*-isomers may display thermal $\tau_{1/2}$'s as high as two years at 25 °C compared to a few hours for the parent *cis*-azobenzene.[26] Within these design boundaries, rationally designed **photoPROTACs** possess important characteristics summarized in **Figure 1B**: Highly stable, inactive *cis*-**photoPROTAC** is isomerized by means of a visible light stimulus to a catalytically active *trans*-**photoPROTAC** which induces polyubiquitination of a protein of interest (POI) by complexation with an E3 ligase. The labeled POI then proceeds to degradation by the proteasome while the *trans*-**photoPROTAC** remains active until isomerization via a second light stimulus of a different wavelength that regenerates the inactive *cis*-**photoPROTAC**.

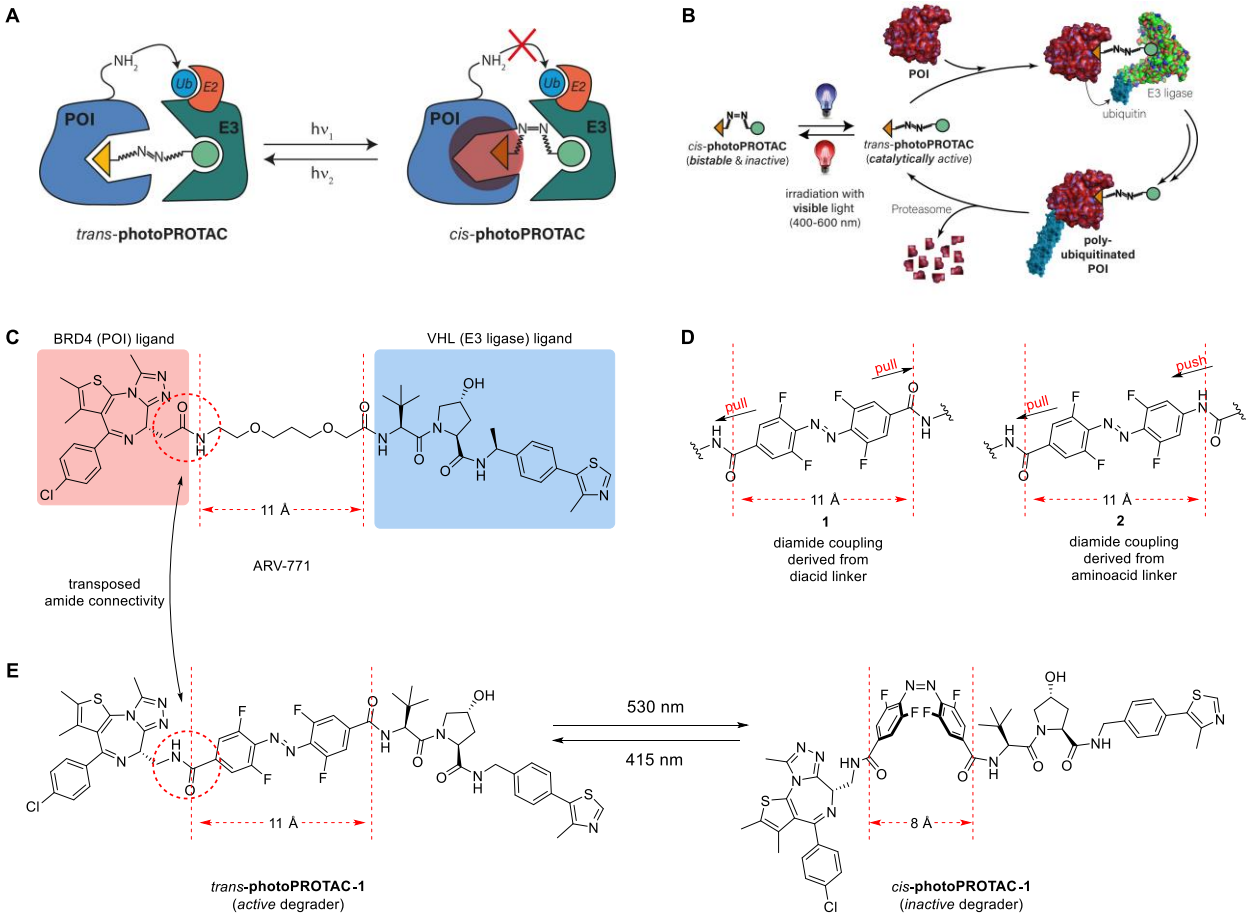

Figure 1: Concept of **photoPROTACs**. **A**: The functional azobenzene handle allows for photo-induced switching between an active *trans*- and inactive *cis*-**photoPROTAC** isomer which is prohibitively short to engage both proteins in a ternary complex. **B**: Features

of **photoPROTACs**: catalytic, bistable and switchable with visible light. **C**: Structure of highly active BET protein degrader ARV-771 displaying a maximal distance of 11 Å between both warhead moieties. **D**: "pull-pull" and "push-pull" modes of modular connectivity for introduction of an *o*-F_4 azobenzene moiety. **E**: Devised BRD4 **photoPROTAC**, representatively shown with "pull-pull" diacid linker. The *trans*-isomer retains the maximal distance displayed by ARV-771 while the *cis*-isomer is considerably shorter.

As a first **photoPROTAC** proof-of-concept, ARV-771[13] (**Figure 1C**) was selected as the lead structure for the generation of a photoswitchable BET protein degrader. To introduce the *o*-F_4-azobenzene fragment within the PROTAC scaffold as part of a highly modular synthesis approach, two different amide linkers (**Figure 1D**) were envisioned involving either a precursor *o*-F_4-azobenzene diacid, as shown embedded in **1**, or, alternatively, an *o*-F_4-azobenzene amino-acid, as shown in **2**. The designed replacement of the oligoether linker in ARV-771 with photoswitchable linkers furnishes the isomeric **photoPROTAC** pair shown in **Figure 1E**, which maintain an optimal distance of 11 Å between both warheads for the putatively active *trans*-**photoPROTAC-1** and diminished distance of 8 Å in *cis*-**photoPROTAC-1**.

Results. Synthetic efforts commenced with the generation of unsymmetrical, aminoacid *o*-F_4-azobenzene linker as shown in **Figure 1D** (right) which had been predicted to possess a *cis*-$\tau_{½}$ of about 80 days.[27] The use of Feringa's method[28] gave access to **6** from diazonium salt **4** and the organolithium derivative derived from protected 3,5-difluoroaniline **5** (**Figure 2A**). Subsequent palladium-catalyzed carbonylative esterification furnished aminoester **7**.[29] Initial efforts to remove the bisallyl protecting group under classical Pd-mediated conditions[30] were not met with success. Instead, ruthenium-catalyzed isomerization and subsequent hydrolysis of the enamine produced gave the targeted aniline **8**.[31] Acetylation of aniline **8** gave **9**, which served as a model to examine bistability. Switching between *trans*-**9** and *cis*-**9** occurred by irradiation at the well-separated n-π^* absorption bands at 415 nm (*cis*-*trans*) and 530 nm (*trans*-*cis*), respectively. Unfortunately, *cis*-**9** generated under 530 nm irradiation quickly isomerized to the thermodynamically more stable *trans*-**9** with a thermal half-life of $\sim$ 2 hours (**Figure 2B**). On the basis of our design criteria, this observation rendered azobenzene linker building block **8** unsuitable. It is important to note that this observation is in line with the general concept of diminished bistability of "push-pull" azobenzenes.[32,33]

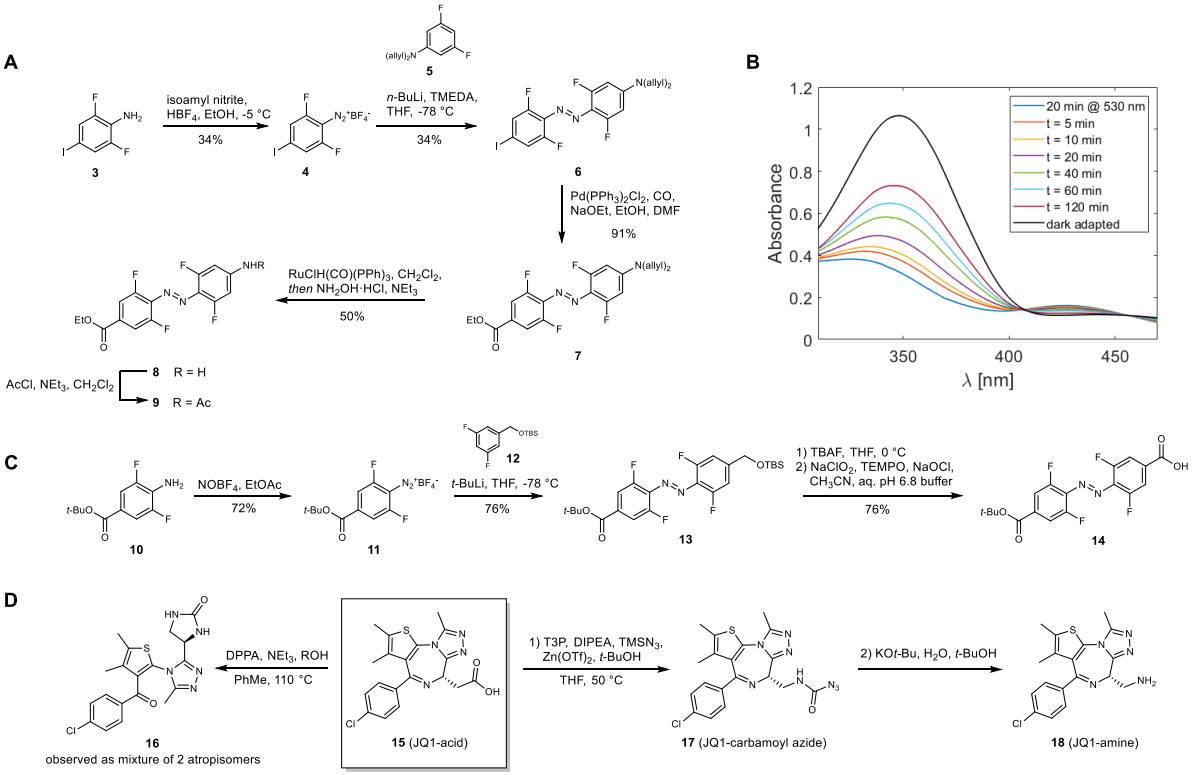

Figure 2: A: Synthetic approach towards unsymmetrical aminoacid azobenzene linker **8**. **B**: Bistability measurement of model substrate **9**, starting with enriched *cis*-**9** (t = 0) after a 20-minute irradiation at 530 nm (50 μM in CH_3CN). **C**: Synthetic approach towards monoprotected diacid azobenzene building block **14**. **D**: Classical Curtius conditions mainly generated urea **16** under reflux conditions, preventing access to **18**. Milder Curtius conditions under Lewis-acid catalysis allow to isolate **17** which could be transfomred into JQ-1 amine **18**.

The results with **9** prompted us to revise the design of the **photoPROTAC** conjugate to include a "pull-pull" system by the introduction of diacid linker as shown for **1** (**Figure 1D/E**), bearing two electron-withdrawing substituents. Notably, this permutation in design necessitated a transposition of the amide bond joining BET protein ligand JQ-1 and the azobenzene linker moiety (**Figure 1C/E**). For ease of handling, generation of building block **14** was targeted, which would allow for facile discrimination of both substitution sites. Aniline **10** was generated in a 3-step sequence starting from 2,6-difluoro-4-iodoaniline (**Figure 2C**). Treatment of **10** with $NOBF_4$ in EtOAc afforded diazonium tetrafluoroborate **11**.[34] The diazonium salt was trapped with lithiated TBS-protected 3,5-difluorobenzylalcohol **12** to furnish unsymmetrically substituted *o*-F_4-azobenzene **13**.[28] After TBS deprotection with TBAF and oxidation[35] of the obtained benzylic alcohol desired bifunctional azobenzene linker **14** was generated.

To synthesize required JQ1-amine **18**, a sequence was devised to convert JQ1-acid **15** to the corresponding amine via Curtius rearrangement. However, under classical conditions, the isocyanate generated could not be trapped by alcohols such as *tert*-butanol or benzyl alcohol but instead led to the formation of urea **16** (**Figure 2D**). We hypothesized that intramolecular reaction of the intermediate isocyanate with the diazepine was leading to complications and examined alternative conditions involving the use of $TMSN_3$ under mild conditions.[36,37] Under these conditions JQ1-carbamoyl azide **17** was isolated, which could then be easily deprotected within minutes by

employing KO*t*-Bu in aq. *t*-BuOH. This facile sequence may be generally applicable with challenging substrates for the Curtius rearrangement.

With all necessary building blocks in hand the desired BRD4-**photoPROTAC-1** was assembled by a series of amide couplings (**Figure 3A**). After coupling of VHL ligand **19** to the azobenzene, the *tert*-butyl ester was hydrolyzed with TFA, and JQ-1 amine **18** was attached furnishing *o*-F_4-azobenzene linked BRD4-**photoPROTAC 1**. Next, the photochemical properties of the conjugate generated were examined. In DMSO, the *cis-trans* switch occurred efficiently by irradiation at 415 nm (**Figure 3B**), producing a photostationary state consisting of 95% *trans*-**photoPROTAC-1** as determined by separation of both isomers via HPLC (**Figure 3C**). As anticipated, irradiation at 530 nm established a photostationary state consisting of 68% *cis*-**photoPROTAC-1**. Importantly, the reported bistability of the "pull-pull" *ortho*-F_4 azobenzene was retained in the **photoPROTAC-1** derivative, and no thermal back-isomerization of *cis*-**photoPROTAC-1** was observed in DMSO, acetonitrile or aq. buffer for several days at 37 °C.

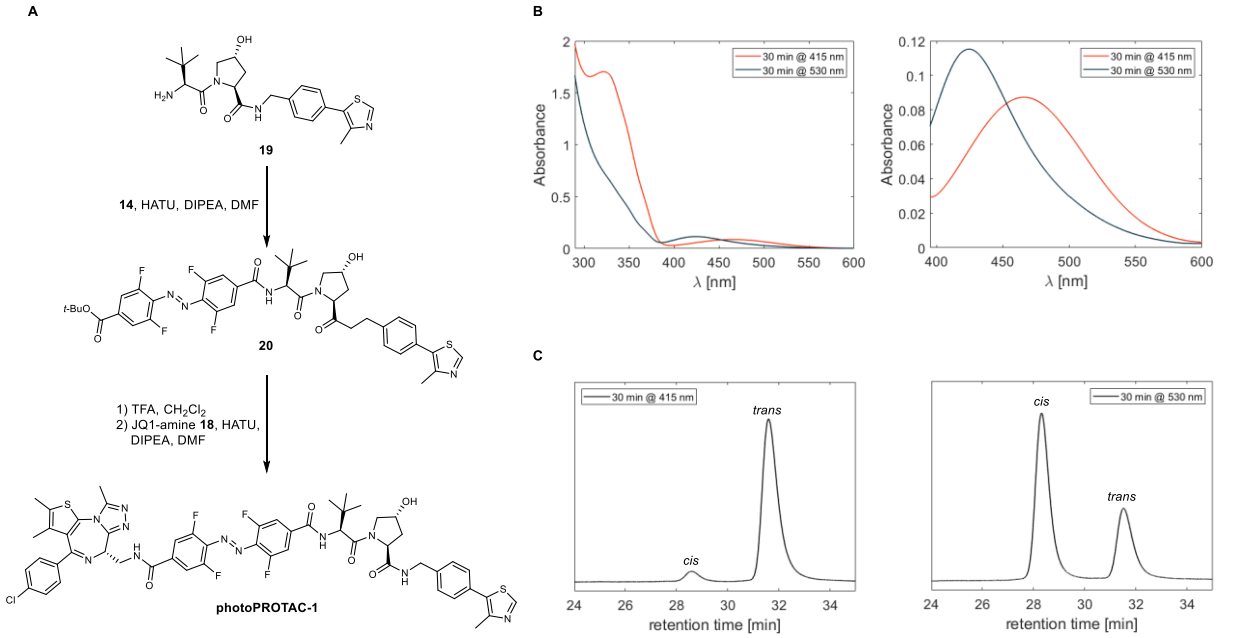

Figure 3: **A**: Modular assembly of **photoPROTAC-1**. **B**: UV-Vis spectra of photoenriched *trans*-**photoPROTAC-1** (415 nm) and *cis*-**photoPROTAC-1** (530 nm) in DMSO. **C**: RP-HPLC chromatograms of photoenriched *trans*-**photoPROTAC-1** (415 nm) and *cis*-**photoPROTAC-1** (530 nm) in DMSO shown at isosbestic wavelength (275 nm in CH_3CN/H_2O).

Having confirmed that **photoPROTAC-1** is efficiently switching between *cis*- and *trans*-configurations upon irradiation with 530 and 415 nm wavelengths, to test our hypothesis, we next carried out biological experiments in Ramos cells. **PhotoPROTAC-1** solutions were irradiated using 415 nm or 530 nm LEDs for initial 20 minutes to obtain *trans*- and *cis*-isomers; after 1-minute rest and brief vortexing, irradiation was continued for another 10 minutes. *Trans*- and *cis*-**photoPROTAC-1** solutions were diluted to desired concentrations and added to Ramos cells. Incubation of *trans*-**photoPROTAC-1** for 6.5 h significantly induced the degradation of BRD2 at low nanomolar concentrations (**Figure 4A**). Conversely, *cis*-**photoPROTAC-1** did not induce degradation of BRD2 in the range of concentrations treated. A longer 18 hr incubation with either *cis*-or *trans*-**photoPROTAC-1** did not improve or affect

the BRD2 degradation efficiencies (**Figure 4B**). Curiously, the data did not show a significant degradation of BRD4 in response to *cis*- or *trans*-**photoPROTAC-1** treatments even though ARV-771 could degrade both BRD4 and BRD2, and with greater potency. Although no structural data is currently available for *trans*-**photoPROTAC-1** bound to BRD4, hypotheses for the observed differential degradation include a gained selectivity of the *trans*-**photoPROTAC-1** towards BRD2 over BRD4 due to the reversed amide bond between JQ-1 and *o*-F_4-azobenzene moiety – a structural feature in contrast with ARV-771 (**Figure 1C and E**). Furthermore, the potential loss of important interactions with BRD4 due to the different positioning of amide bonds in trans-**photoPROTAC-1** might result in a less stable ternary complex, leading to a more rapid dissociation and inefficient ubiquitination and proteasomal degradation of BRD4. Overall, these data suggested that the *o*-F_4-azobenzene moiety within **photoPROTAC-1** allows rapid interconversion between active *trans*-**photoPROTAC-1** and inactive *cis*-**photoPROTAC-1.** Concordantly, the biological data indicate efficient degradation of BRD2 by *trans*-**photoPROTAC-1** and minimum degradation by *cis*-**photoPROTAC-1**.

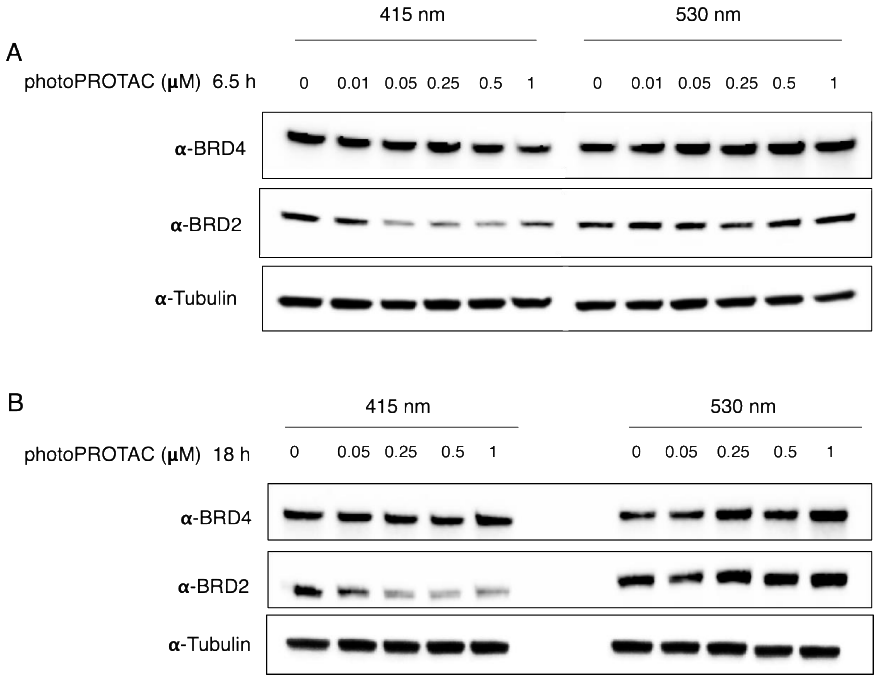

Figure 4: PhotoPROTAC-1 can be converted to active *trans*- and inactive *cis*-isomers to induce differential degradation of BRD2. **PhotoPROTAC-1** working-solutions were irradiated for 30 minutes using 415 nm or 530 nm LEDs and added to Ramos cells at varying concentrations. **A:** Cells were incubated in dark for 6.5 h or **B:** 18 h prior to cell lysis. Treatment of active t*rans*-**photoPROTAC** induce significant BRD2 degradation within 6.5 h where inactive *cis*-**photoPROTAC-1** did not show significant effect on BRD2 levels. BRD4 degradation was not observed under indicated conditions.

Next, to test the reversible photoswitching between the *cis*-**photoPROTAC-1** and *trans*-**photoPROTAC-1**, we performed a two-step irradiation process using both 415 nm and 530 nm LEDs. Initial 415 nm and 530 nm irradiations were carried out separately for 30 minutes to obtain active *trans*-**photoPROTAC-1** and inactive *cis*-**photoPROTAC-1**, respectively. *Trans*-**photoPROTAC-1** and *cis*-**photoPROTAC-1** were then subdivided (50:50) into two tubes each. One tube of each **photoPROTAC-1** isomer was set aside; while the remaining tube of *trans*-**photoPROTAC-1** was subjected to a second round of irradiation at 530 nm, and the remaining tube of *cis*-

photoPROTAC-1 was exposed to the 415 nm LED. To assess the reversible photo-isomerization of the **photoPROTACs**, Ramos cells were then separately treated with varying concentrations of either singly irradiated (415 nm: *trans*-**photoPROTAC-1** or 530 nm: *cis*-**photoPROTAC-1**) or doubly irradiated (530/415 nm: *trans*-**photoPROTAC-1** or 415/530 nm: *cis*-**photoPROTAC-1**) **photoPROTACs**. After 18 h incubation with **photoPROTACs** derived from different combinations of irradiations, cells were lysed and analyzed for the BRD4 and BRD2 levels. In line with the previous experiment (**Figure 4**), similar BRD4/2 degradation patterns were observed for the *trans*-**photoPROTAC-1** and *cis*-**photoPROTAC-1** that were obtained through single irradiation (**Figure 5**, 415 nm or 530 nm). As regards the double-irradiated **photoPROTACs** (**Figure 5**, 530/415 nm or 415/530 nm), the data demonstrate a complete reversal of their degradation potential following the second irradiation (i.e. 530 nm followed by 415 nm LEDs or vice versa) suggesting that *o*-F_4-azobenzene moiety can be successfully adopted into PROTAC linkers for light-induced, spatiotemporal control of target protein degradation.

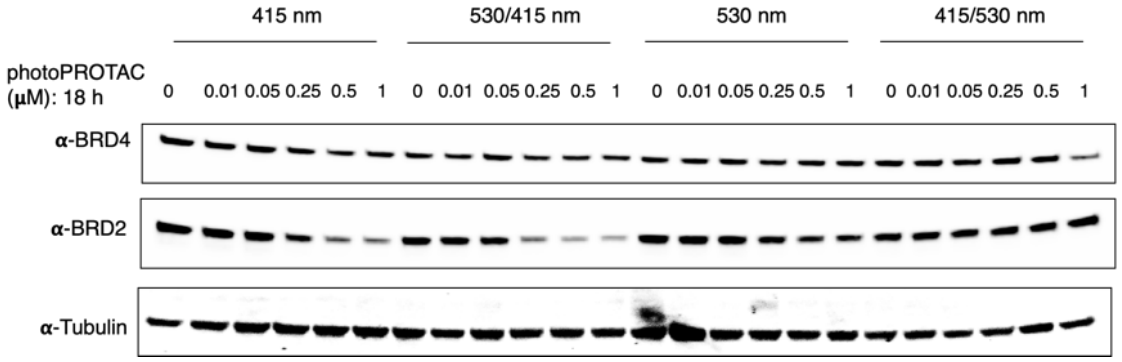

Figure 5: PhotoPROTACs are dynamically interchangeable between active *trans*- and inactive *cis*-configurations. **PhotoPROTAC-1** working solutions were initially irradiated with 415 nm or 530 nm LEDs followed by second irradiation using 530 nm or 415 nm (415/530 nm and 530/415 nm) to reverse the initial configurations. Treatment of singly irradiated *trans*-**photoPROTAC-1** (415 nm) induced a significant BRD2 degradation relative to the *cis*-**photoPROTAC-1** (530 nm) whereas no significant BRD4 degradation was observed in response to both *trans*- and *cis*-p**hotoPROTAC-1**. Second irradiation with either 530 nm or 415 nm significantly shifted the biologically active *trans*-isomer to inactive *cis*-isomer and vice versa.

Our data indicate that initial irradiation of **photoPROTAC-1** is sufficient to yield successful spatiotemporal control of **photoPROTAC-1** and avoids laborious continuous-irradiation efforts to induce the photoswitching between active and inactive states of PROTACs. Moreover, sustained BRD2 degradation after an 18 hour incubation (**Figure 4B**) is an indication of the bistability of *o*-F_4-azobenzene containing **photoPROTAC-1**. Had the *trans*-isomer switched back to the cis-isomer, persistent BRD2 degradation would not have been prominent considering the significant resynthesis of BRD proteins that occurs as a feedback mechanism in response to inhibition (**Figure 4A** and **4B**, 530 nm treated cells).[38] Hence, the current approach not only provides robust control over induced-degradation but also offers the advantage of not exposing cells to continuous irradiation. Taken together, our data provide evidence to support the fact that use of *o*-F_4-azobenzene moiety towards PROTAC design, provides a powerful strategy to spatiotemporally control PROTAC activity with a single initial irradiation step.

Outlook. Bistable heterodiazocine motifs, displaying >99% *cis*-content in the dark with stable *trans*-isomers bearing thermal half-lives of several days are promising candidates that may be amalgamated with our overarching strategy to generate *cis*-inactive **photoPROTACs**.[39] Future approaches could include azobenzenes sufficiently red-shifted to allow irradiation in NIR/IR window for optimal tissue penetration.[40,41] Additionally, taking advantage of two-photon excitation processes may further enable switching in a more favorable window.[42,27]

Applications of our **photoPROTAC** method targeting proteins beyond BET domains are currently under investigation and will be reported in due course. This also includes engagement of other E3 ligases such as cereblon or MDM2. Moreover, **photoPROTACs** may serve as a platform for aggressively targeting central parts of the cell machinery with high resolution, for example for the degradation of anti-apoptotic proteins. Dilution via diffusion of the on-site activated *trans*-**photoPROTAC** may suffice to prevent off-target effects. But, for even higher resolution, back-switching of the activated *trans*-**photoPROTAC** to the inactive *azo*-*cis*-isomer by a second optical fiber light source in a defined distance to the applied site can be envisioned. This is an advantage over conventional photocaging strategies which release active drugs only irreversibly.

While in the process of preparing this manuscript, we became aware of a preprint demonstrating an alternative approach by generating *cis*-active photoswitchable PROTACs.[43] In their complementary approach, Trauner *et al.* introduced azobenzene moieties to ligands of E3 ligase cereblon. In contrast to our bistable system, their strategy necessitates continued light pulses at 390 nm to induce prolonged degradation otherwise their degrader remains inactive in the dark.

Conclusion. The combination of two recently emerging areas in drug discovery, namely photopharmacology and small molecule degraders, have led us to develop the concept of photoswitchable, bistable **photoPROTACs** with potentially far reaching implications for manifold applications. In combination with modern methods of proteomics, **photoPROTACs** offer further opportunity for studying downstream effects of signaling pathways which are yet insufficiently understood.[44] More broadly, it should be noted that spatiotemporal activation/deactivation of photoswitchable PROTACs by a single irradiation event may find use in novel therapeutics.

Acknowledgements

C.M.C. gratefully acknowledges support from the NIH (R35 CA197589). C.M.C. is a shareholder in and consultant to Arvinas, Inc., which partially supported this work. P.P. acknowledges a fellowship of the Stipendienfonds Schweizerische Chemische Industrie (SSCI). John Hines is acknowledged for assistance in editing the manuscript.

References

1. Lai, A. C. & Crews, C. M. Induced protein degradation: An emerging drug discovery paradigm. *Nat. Rev. Drug Discov.* **16**, 101–114 (2017).
2. Burslem, G. M. & Crews, C. M. Small-Molecule Modulation of Protein Homeostasis. *Chem. Rev.* **117**, 11269–11301 (2017).

3. Buhimschi, A. D. *et al.* Targeting the C481S Ibrutinib-Resistance Mutation in Bruton's Tyrosine Kinase Using PROTAC-Mediated Degradation. *Biochemistry* **57**, 3564–3575 (2018).
4. Souza, A. *et al.* Phthalimide conjugation as a strategy for in vivo target protein degradation. *Science* **348**, 1376–1381 (2015).
5. Lu, J. *et al.* Hijacking the E3 Ubiquitin Ligase Cereblon to Efficiently Target BRD4. *Chem. Biol.* **22**, 755–763 (2015).
6. Liang, Y. *et al.* Pharmacological perturbation of CDK9 using selective CDK9 inhibition or degradation. *Nat. Chem. Biol.* **14**, 163–170 (2017).
7. Perry, J. A. *et al.* Functional TRIM24 degrader via conjugation of ineffectual bromodomain and VHL ligands. *Nat. Chem. Biol.* **14**, 405–412 (2018).
8. McQuaid, D. C. *et al.* The Advantages of Targeted Protein Degradation Over Inhibition: An RTK Case Study. *Cell Chem. Biol.* **25**, 67-77.e3 (2017).
9. Nowak, R. P. *et al.* Chemically Induced Degradation of Anaplastic Lymphoma Kinase (ALK). *J. Med. Chem.* **61**, 4249–4255 (2018).
10. Bondeson, D. P. *et al.* Catalytic in vivo protein knockdown by small-molecule PROTACs. *Nat. Chem. Biol.* **11**, 611–617 (2015).
11. Silva, M. C. *et al.* Targeted degradation of aberrant tau in frontotemporal dementia patient-derived neuronal cell models. *Elife* **8**, 8:e45457 (2019).
12. Saenz, D. T. *et al.* Novel BET protein proteolysis-Targeting chimera exerts superior lethal activity than bromodomain inhibitor (BETi) against post-myeloproliferative neoplasm secondary (s) AML cells. *Leukemia* **31**, 1951–1961 (2017).
13. Dong, H. *et al.* PROTAC-induced BET protein degradation as a therapy for castration-resistant prostate cancer. *Proc. Natl. Acad. Sci.* **113**, 7124–7129 (2016).
14. Nalawansha, D. A. *et al.* Targeted Protein Internalization and Degradation by ENDosome TArgeting Chimeras (ENDTACs). *ACS Cent. Sci.* acscentsci.9b00224 (2019). doi:10.1021/acscentsci.9b00224
15. Banik, S. M., Pedram, K., Wisnovsky, S., Riley, N. M. & Bertozzi, C. R. LysosomeTargeting Chimeras (LYTACs) for the Degradation of Secreted and Membrane Proteins. *ChemRxiv* **preprint**, 10.26434/chemrxiv.7927061 (2019).
16. Hines, J., Gough, J. D., Corson, T. W. & Crews, C. M. Posttranslational protein knockdown coupled to receptor tyrosine kinase activation with phosphoPROTACs. *Proc. Natl. Acad. Sci.* **110**, 8942–8947 (2013).
17. Delacour, Q. *et al.* Light-Activated Proteolysis for the Spatiotemporal Control of Proteins. *ACS Chem. Biol.* **10**, 1643–1647 (2015).
18. Bonger, K. M., Rakhit, R., Payumo, A. Y., Chen, J. K. & Wandless, T. J. General Method for Regulating Protein Stability with Light. *ACS Chem. Biol.* **9**, 111–115 (2014).
19. Velema, W. A., Szymanski, W. & Feringa, B. L. Photopharmacology: Beyond proof of principle. *J. Am. Chem.*

Soc. **136**, 2178–2191 (2014).

20. Westphal, M. V. *et al.* Synthesis of Photoswitchable Δ9-Tetrahydrocannabinol Derivatives Enables Optical Control of Cannabinoid Receptor 1 Signaling. *J. Am. Chem. Soc.* **139**, 18206–18212 (2017).
21. Hüll, K., Morstein, J. & Trauner, D. In Vivo Photopharmacology. *Chem. Rev.* **118**, 10710–10747 (2018).
22. Bondeson, D. P. *et al.* Lessons in PROTAC Design from Selective Degradation with a Promiscuous Warhead. *Cell Chem. Biol.* **25**, 78-87.e5 (2018).
23. Smith, B. E. *et al.* Differential PROTAC substrate specificity dictated by orientation of recruited E3 ligase. *Nat. Commun.* **10**, (2019).
24. Zhou, B. *et al.* Discovery of a Small-Molecule Degrader of Bromodomain and Extra-Terminal (BET) Proteins with Picomolar Cellular Potencies and Capable of Achieving Tumor Regression. *J. Med. Chem.* **61**, 462–481 (2018).
25. Bléger, D., Schwarz, J., Brouwer, A. M. & Hecht, S. O -fluoroazobenzenes as readily synthesized photoswitches offering nearly quantitative two-way isomerization with visible light. *J. Am. Chem. Soc.* **134**, 20597–20600 (2012).
26. Knie, C. *et al.* Ortho-Fluoroazobenzenes: Visible Light Switches with Very Long-Lived Z Isomers. *Chem. - A Eur. J.* **20**, 16492–16501 (2014).
27. Cabré, G. *et al.* Rationally designed azobenzene photoswitches for efficient two-photon neuronal excitation. *Nat. Commun.* **10**, (2019).
28. Hansen, M. J., Lerch, M. M., Szymanski, W. & Feringa, B. L. Direct and Versatile Synthesis of Red-Shifted Azobenzenes. *Angew. Chemie - Int. Ed.* **55**, 13514–13518 (2016).
29. Hu, Y. *et al.* Base-induced mechanistic variation in palladium-catalyzed carbonylation of aryl iodides. *J. Am. Chem. Soc.* **132**, 3153–3158 (2010).
30. Garro-Helion, F., Merzouk, A. & Guibé, F. Mild and Selective Palladium(0)-Catalyzed Deallylation of Allylic Amines. Allylamine and Diallylamine as Very Convenient Ammonia Equivalents for the Synthesis of Primary Amines. *Journal of Organic Chemistry* **58**, 6109–6113 (1993).
31. Lutz, T. A., Spanner, P. & Wanner, K. T. A general approach to substituted diphenyldiazenes. *Tetrahedron* **72**, 1579–1589 (2016).
32. Dong, M., Babalhavaeji, A., Samanta, S., Beharry, A. A. & Woolley, G. A. Red-Shifting Azobenzene Photoswitches for in Vivo Use. *Acc. Chem. Res.* **48**, 2662–2670 (2015).
33. Garcia-Amorós, J., Díaz-Lobo, M., Nonell, S. & Velasco, D. Fastest thermal isomerization of an azobenzene for nanosecond photoswitching applications under physiological conditions. *Angew. Chemie - Int. Ed.* **51**, 12820–12823 (2012).
34. Wannagat, U. & Hohlstein, G. Zur Fluorierung mit Nitrosyl-tetrafluoro-borat. *Chem. Ber.* **88**, 1839–1846 (1955).
35. Mano, E. *et al.* Oxidation of Primary Alcohols to Carboxylic Acids with Sodium Chlorite Catalyzed by TEMPO

and Bleach. *J. Org. Chem.* **64**, 2564–2566 (2002).

36. Lebel, H. & Leogane, O. Boc-protected amines via a mild and efficient one-pot curtius rearrangement. *Org. Lett.* **7**, 4107–4110 (2005).
37. Augustine, J. K. *et al.* Propylphosphonic anhydride (T3P®)-mediated one-pot rearrangement of carboxylic acids to carbamates. *Synthesis (Stuttg).* 1477–1483 (2011). doi:10.1055/s-0030-1259964
38. Riching, K. M. *et al.* Quantitative Live-Cell Kinetic Degradation and Mechanistic Profiling of PROTAC Mode of Action. *ACS Chem. Biol.* **13**, 2758–2770 (2018).
39. Hammerich, M. *et al.* Heterodiazocines: Synthesis and Photochromic Properties, Trans to Cis Switching within the Bio-optical Window. *J. Am. Chem. Soc.* **138**, 13111–13114 (2016).
40. Profio, A. E. Light transport in tissue. *Appl. Opt.* **28**, 2216–22 (1989).
41. Zhang, H. *et al.* Penetration depth of photons in biological tissues from hyperspectral imaging in shortwave infrared in transmission and reflection geometries. *J. Biomed. Opt.* **21**, 126006 (2016).
42. Passlick, S., Richers, M. T. & Ellis-Davies, G. C. R. Thermodynamically Stable, Photoreversible Pharmacology in Neurons with One- and Two-Photon Excitation. *Angew. Chemie - Int. Ed.* **57**, 12554–12557 (2018).
43. Reynders, M. *et al.* PHOTACs Enable Optical Control of Protein Degradation. *ChemRxiv* **preprint**, 10.26434/chemrxiv.8206688 (2019).
44. Greene, C. S. *et al.* Oncogenic Signaling Pathways in The Cancer Genome Atlas. *Cell* **173**, 321-337.e10 (2018).